INVESTIGATION OF THE PARTICLE TRANSPORT IN COMPRESSIBLE VORTICES PRODUCED BY SHOCK DIFFRACTION

W. JÄGER
French-German Research Institute Saint-Louis (ISL)
68301 Saint-Louis, France

Abstract

The transport of particles in a compressible, two-dimensional vortex behind an edge in a shock-tube is examined both experimentally and theoretically. In order to point out the limits of laser anemometry, the deviations of the particle movement from the vortex movement dependent on the particle material are calculated numerically as well as experimentally, and presented with a new optical measuring technique for the investigation of velocity distributions, by means of Doppler-pictures.

Introduction

The determination of flow velocities is made more and more with the help of the optical Doppler-effect. Because of the Doppler-shifted frequency of light scattered through dust particles, the velocity of the particles added to the flow can be ascertained. With sufficiently small particles, the particle velocity is practically the same as the flow velocity. The measuring method fails if too high gradients of velocity in the flow area occur. Measurements of velocity jumps of weak shock waves by George[1] give an impression of this. The velocity jumps were registered with two different measuring techniques with a Doppler-interference velocimeter and with a Mach-Zehnder interferometer. Figure 1 shows that the maximum of the velocity jump in a spark is not reached before the double or treble time in the measurement with the velocimeter and the amplitude is about 10% smaller than with the interferometer measurement.

The noise of supersonic jets is emitted in form of rather regular Machwaves (Oertel et al.[7]). The question is, how the Machwaves depend on the characteristics of the jet and the ambient gas, and what is the reason for their having nearly equal angles. With an interferometer for taking x,t-streak records, particularly clear traces informed about the speeds of the mixing layer structures at the origins of the Machwaves. Immobilizations on appropriately moving film (Fig.2) revealed the fact that travelling Machwaves having a preferred angle do also exist inside the jet. With different measuring techniques several surprisingly simple similarity laws have been found which have finally led to the proposal of suppressing the Machwaves by means of a hot subsonic envelope. It could

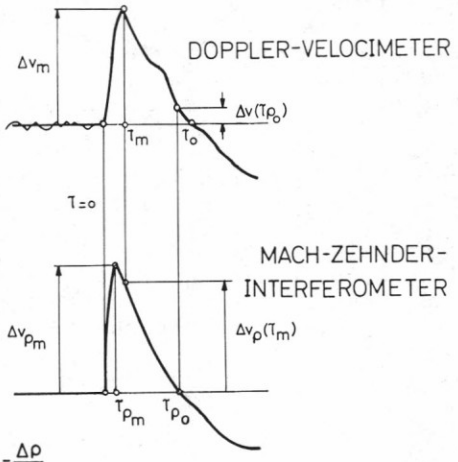

$$\frac{\Delta v}{a} = \frac{\Delta \rho}{\rho}$$

$\frac{\Delta v_m}{m\,s}$	$\frac{\Delta v_{\rho m}}{m\,s}$	$\frac{\Delta v_m}{\Delta v_{\rho m}}$	$\frac{\lvert\Delta v_m - \Delta v_{\rho m}\rvert}{\Delta v_{\rho m}}$	$\frac{\tau_m}{us}$	$\frac{\tau_{\rho m}}{us}$	$\frac{\tau_m - \tau_{\rho m}}{\tau_{\rho_m}}$
14.23	17.48	0.81	0.19	6.2	3.0	1.07
14.98	16.97	0.88	0.12	6.0	2.0	2.0
17.98	17.49	1.03	0.06	6.0	3.0	1.07
15.35	16.47	0.93	0.07	5.8	2.0	1.90
15.01	15.53	0.97	0.03	5.0	2.0	1.50
Mean values						
15.51	16.79	0.92	0.09	5.80	2.40	1.51

Fig.1: Measurements of the velocity jump of a weak shock wave (George[1])

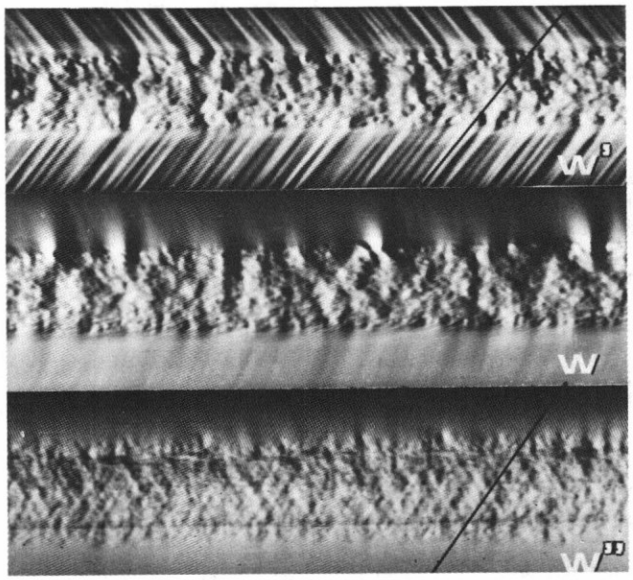

Fig.2: Coherent structures of a supersonic jet (Oertel et al.[7])

be shown that this method works. But the reason for the simple relations is still unknown. The correlation functions measured with two velocimeters do not support the assumption of strong circumferential coherent structures being the origin of the Machwaves. This failure may perhaps be due to the tracer inertia.

The aim of these investigations is to get knowledge about the dynamics of gases charged with dust and to show the limits of laser-anemometry. The question of whether turbulent flows, especially flows in boundary and mixing layers, can be made visible and measured through dust transport, was to be clarified. Furthermore it was to be shown what streaklines state about a flow, particularly when the particles cannot follow the flow. Therefore the particle transport in a compressible, approximately two-dimensional vortex behind an edge in a shock tube is examined. Figure 3 shows in the upper part the measuring chamber with the built-in model.

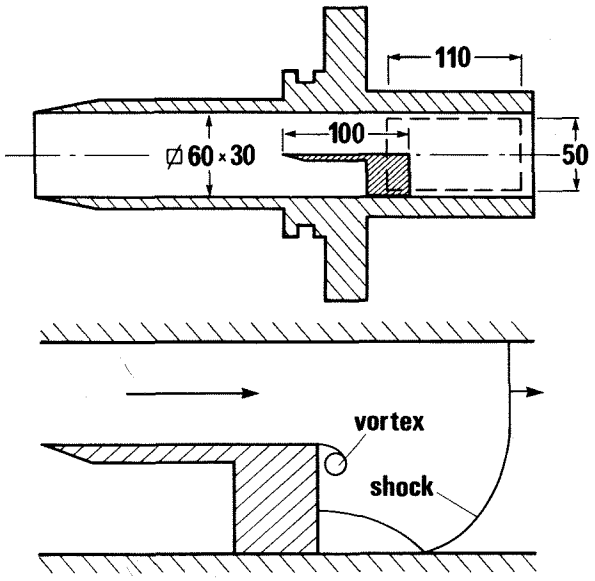

Fig.3: Test chamber

The shock Mach number is 1.2 to 1.6 in the experiments presented here, and the shock produces on the model edge a vortex which moves downstream under a certain angle and thereby grows, as is represented in principle in the lower part of Fig.3. The results of the measurements are compared with the works by Howard and Matthews[2] and Rott [3]. With the help of these works, the particle movement in the vortex can approximately be numerically calculated.

Theory

Howard and Matthews proceed from the assumptions that the vortex discharge is a symmetrical and pseudostationary problem in which the flow variables only depend on one variable, namely the quotient from the vortex radius r and the time t, when the coordinate system moves with the vortex. In addition they assume a homoentrope flow. Leaving the vortex core out of consideration they get from the continuity and momentum equations the flow variables in the vortex as a function of the vortex radius r and the time t, as well as two parameters which represent a measurement for the vortex size and intensity respectively:

$$T;v = f(r,t,r_I,\beta) \ .$$

Rott is concerned with the growth of the vortex and its movement downstream. By neglecting viscosity and heat conduction and in the case of incompressible flow, he gets from the potential equation a relation for the quotient of the distance a of the vortex from the edge and the speed of sound c_2 multiplied by the time t as a function of the Mach number and three angles, that is the model angle, the position angle of the model in the flow and the angle between free flow and vortex motion:

$$\sigma = \frac{a}{c_2 t} = f(M,\varepsilon,\alpha,\psi) \ .$$

Thus the movement of the idealized vortex is fully described. Scattered particles are now added to the flow. For this we assume that the particles follow the free stream without slippage. Besides this, the particles should have a spherical contour and a fixed, known diameter. In the first approximation, the validity of the Stokes law can be assumed. The particle movement is approximately calculated over a balance of forces, as a function of the particle size as well as of the flow data. So the radial velocity of the particles over their position in the vortex can be shown in a diagram, with the particle size R as parameter (Fig.4).

It can be recognized that smaller particles follow the vortex movement better; the radial velocity is small. But even the smallest particles withdraw from the vortex centre. Here the problems with the methods of measuring diffused light become clear. On the one hand, the particles should be large e.g. 1 µm, in order to retain an intensive signal, but on the other hand they should be small, to some extent substantially smaller than 1 µm, so that they can follow the flow extensively. The particle movement in the vortex can be approximately numerically simulated for different particle sizes. The particle movements in two like vortices are represented in Fig.5, firstly for particles with the radius 0.25 µm and secondly for R = 0.75 µm. The flow, coming from the left, has a Mach number of approximately 0.5. The continuous lines represent the lines connecting the starting positions of the particles with their final positions during a small time interval Δt. It is noticeable that the inner area of the vortex, where no particles are, gets considerably bigger with increasing particle size.

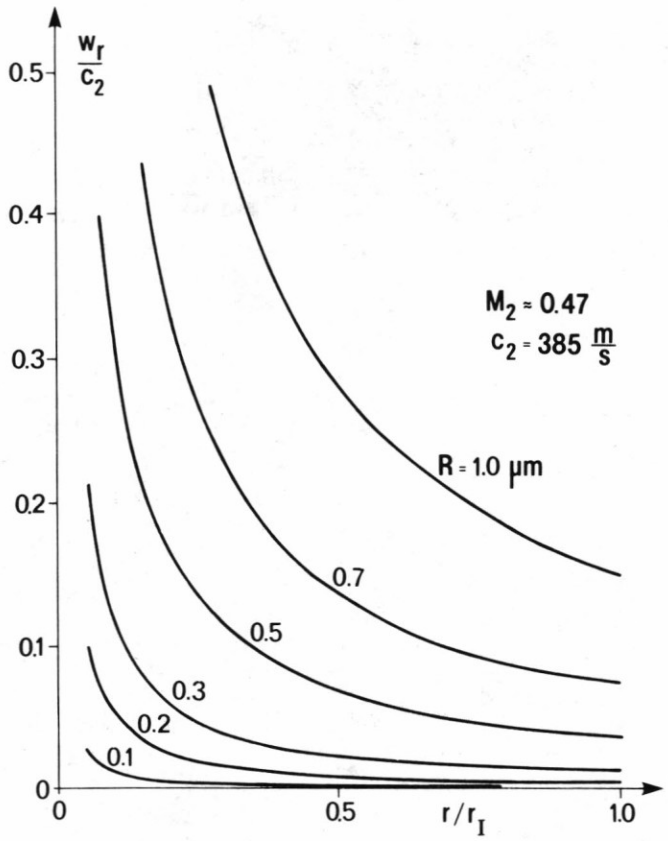

Fig.4: Radial velocity of particles in a vortex ($\rho = 3000\ kg/m^3$)

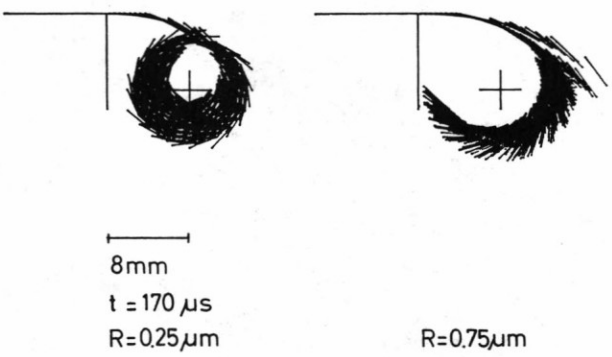

Fig.5: Numerical simulation of particle movement in a vortex

In Figure 6 particle paths and streaklines are shown for particles of differing size. The flow conditions are the same for the three particle sizes observed. A particle which is joined to the flow shortly after the shock wave has run over the edge, describes the path shown on the left of the picture. With increasing size, the particle distances itself from the vortex centre and then no longer follows the movement of the vortex. In the case of $R \approx 0$ the theoretical relations no longer hold, but in this way an approximation of the actual vortex movement is conveyed. It becomes clear that velocity measurements depending on the choice of particles must

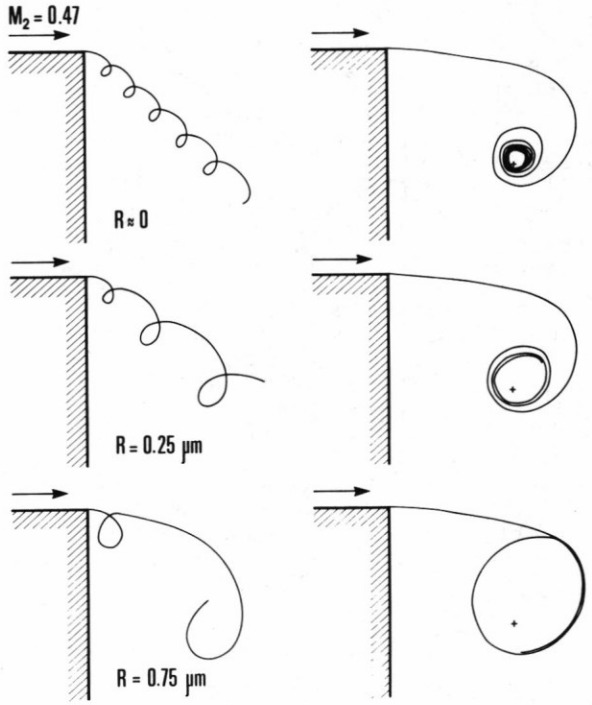

Fig.6: Particle paths and streaklines of particles of different size

lead to differing results. On the right-hand of Fig.6, streaklines are represented. On the basis of these lines it can be recognized how great the deviations from the actual vortex are, if too large particles are chosen. Since the flow processes are very often visualized by streaklines, it must be critically considered what the flow looks like in reality.

Experiment

In Figure 7 we see a vortex with TiO_2 particles at two times, visualized by a shadow method. The Mach number M_2 is just 0.56. The flow with N_2 comes from the left. The interior of the vortex is almost devoid of particles. They cannot follow the vortex movement, which is also shown by the numerical simulation. In comparison

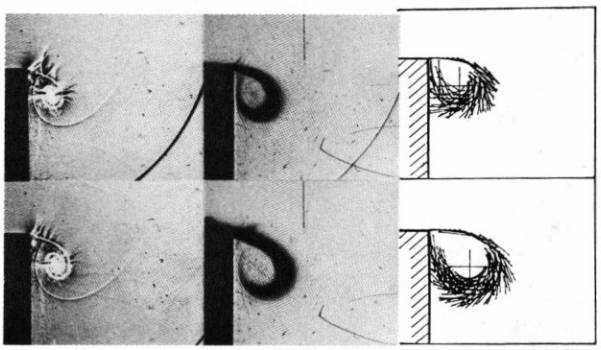

Fig.7: Shadow graphs of vortices at two times without and with TiO_2-particles (M-0.56) | Vectorfields of TiO_2-particle velocities

to this, the vortex without particles is only half as big as the vortex with particles.

For the local measurements of flow velocities, a laser-Doppler velocimeter with a Michelson interferometer is used, which was developed in our department of the ISL. In Fig.8 the principle drawing of the optical set-up can be seen. The Doppler-measurement consists here in a spectrometric determination of the wavelength shift. Laser light illumines the measuring point and is scattered there on the particles. The Doppler-shifted scattered light is focused on an optical fiber with an objective and is thus transported into the spectrometer. The optical path of one of the two interferometer arms is extended with a glass block. A path difference $\Delta\Phi$ makes the interferences dependent on the wavelength and so renders the measuring of wavelength changes possible. The modulation of the intensity P is

$$P = P_0 \cos^2(\pi \frac{\Delta\Phi}{\lambda})$$

with the two-beam interference. If we derive by the wavelength λ, it follows:

$$\frac{dP/P_0}{d\lambda/\lambda} = \pi \frac{\Delta\Phi}{\lambda} \sin(2\pi \frac{\Delta\Phi}{\lambda}) .$$

If $\Delta\Phi$ is chosen very large against the wavelength λ, then a great sensitivity of P compared with small wavelength changes is received. The signal is connected linearly to the velocity component. For further details, see the works of Smeets and George[4] [5].

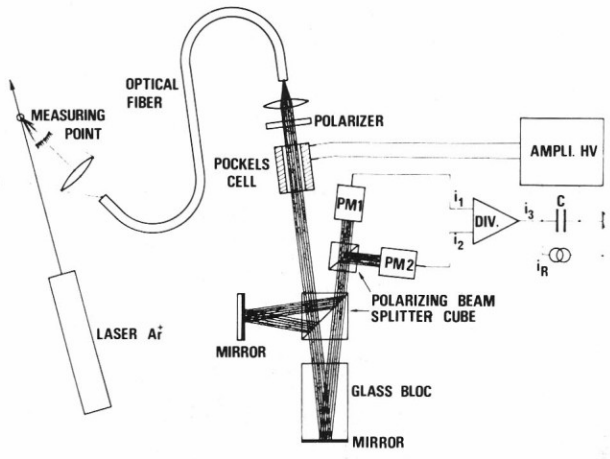

Fig.8: Principle sketch of the laser velocimeter

Fig. 9 shows a velocity signal measured with the velocimeter. The measuring point lies 7 mm downstream and 10 mm below the edge. The shock Mach number is 1.4. The horizontal velocity component of smoke particles is measured. The incident shock leads to a jump in velocity. The consequent vortex, the centre of which runs past above the measuring point, slowly turns the flow direction around. Below the vortex

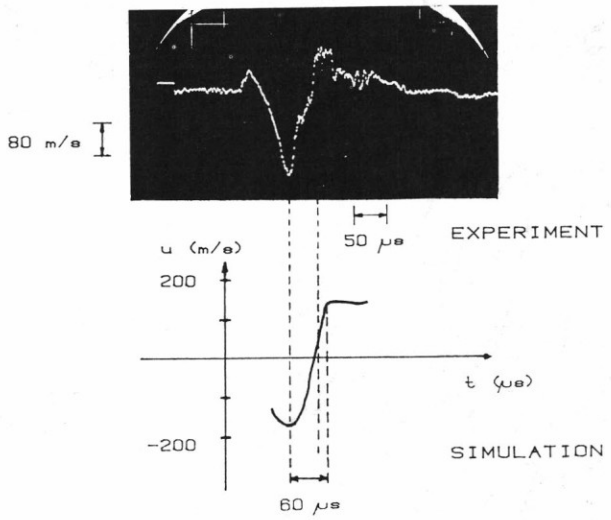

Fig.9: Measured and simulated velocity signals

centre is a back-flow. After reaching the minimum, the velocity increases again, and the measuring place shifts upwards in the vortex.Finally the shock reflected on the wall of the measuring chamber collapses and terminates the experiment. A comparison with the calculation shows the same course for the horizontal velocity component. Since the simulation only covers the vortex flow, no shock waves occur. The vortex reaches the measuring place, the velocity passes through a minimum, turns around, and finally the vortex leaves the measuring place. In the experiment, the velocity change from the minimum to the maximum is 300 m/s, in the calculation for smoke particles it is 310 m/s. The velocity inversion is completed approximately 10 µs faster in the experiment.

With instationary flow problems it is often not the velocity at a certain point as a function of the time which is of interest, but rather the velocity distribution in the flow area at a fixed time. Up to now a velocity picture could only be realised by a multitude of separate measurements. The development of the photographic technique of a so-called Doppler-picture was recently undertaken in our department of the ISL. This method can be applied in particular for investigations at the vortex. The experimental set-up is shown in Fig.10. The basic set-up corresponds to the concept of the Doppler-velocimeter previously described. An optical system which focusses the object onto the mirrors M1 and M2, forms the entry into the interferometer. The splitting of the incident scattered lights follows over a beam-splitter cube. Both mirrors, and thus also the object, are shown over a lens onto a film. If the mirror M1 is turned by a small angle α, then Fizeau-fringes emerge in the plane of the mirrors, parallel to the axis of rotation. A given fringe-pattern is transferred into another

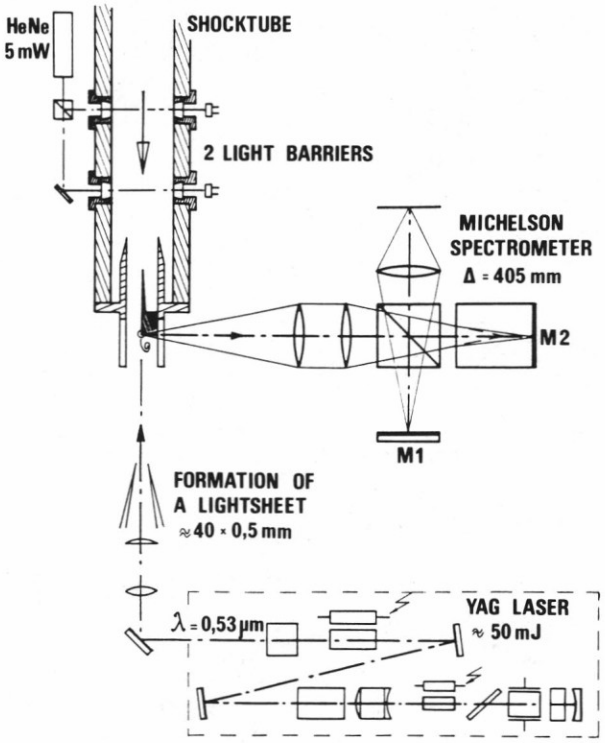

Fig.10: Doppler-picture of a vortex, optical set-up

fringe-pattern by a wavelength change. As has already been shown, the wavelength sensitivity depends on the path difference of the two interferometer arms and thus on the thickness of the glass block. The evaluation of a Doppler-picture is made simply. A wavelength change effects a fringe shift. The wavelength change $\Delta\lambda$ can be directly calculated by measuring the fringe shift Δs and thus also the velocity change:

$$\frac{\Delta u}{c} = \frac{\Delta s}{\Delta\Phi/\lambda} \cdot \frac{1}{\cos\gamma_1 + \cos\gamma_2}$$

with c = light speed; γ_1 = angle between flow direction and lighting direction; γ_2 = angle between flow direction and direction of observation. Further details are described in the work of Oertel et al.[6].

In Fig. 11 four examples of Doppler-pictures of a vortex at different times are represented. The flow comes from the left with a shock Mach number of 1.5 in N_2. Smoke particles are added to the flow. The undisturbed interference fringe-pattern lies parallel to the model edge. The shift of the interference fringes in the vortex can be clearly recognized. With this method of measuring, we also receive information about the particle distribution, as well as about velocity distribution in the vortex. Again it can be recognized that the interior of the vortex is practically free of particles. So measuring the velocity in this area is in principle hardly possible.

To compare this method with the local velocimeter method we determine the veloc-

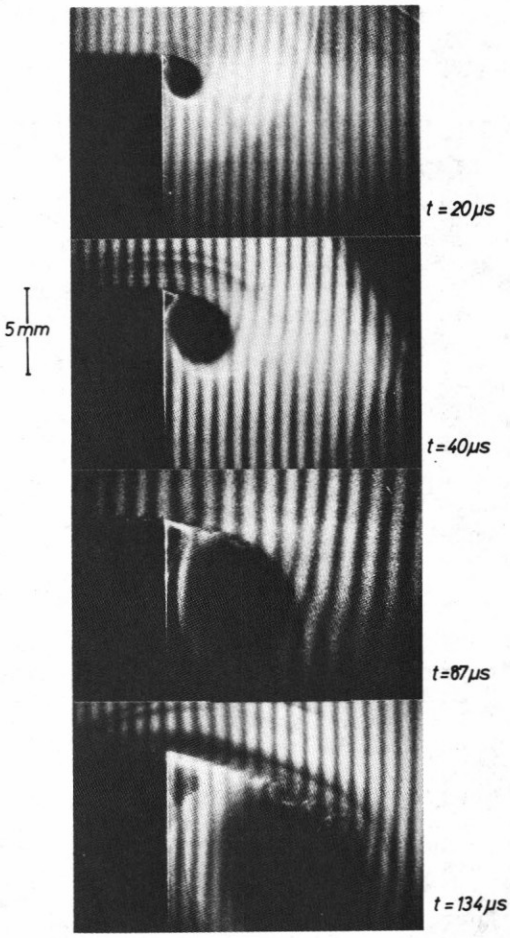

Fig.11: Doppler-pictures of a vortex

ities of the four Doppler-pictures at an adequate place (Fig.12). This place was 2 mm downstream and 4 mm below the edge. Both techniques show comparable results with a systematical error of about 10 µs, perhaps coming from the t = 0 determination.

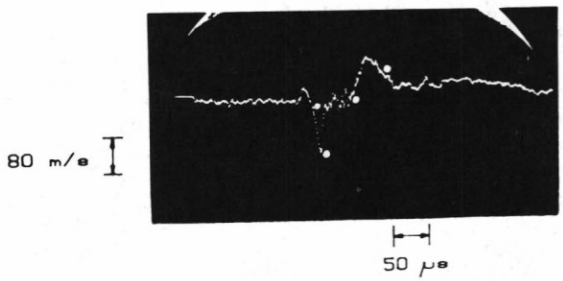

Fig.12: Comparison of Doppler-picture and velocimeter measurements

Concluding remarks

With the theories of Howard and Matthews as well as Rott, the flow of a vortex behind an edge is described in approximation. Thus the particle movement depending on the particle size and density can be calculated by applying the law of Stokes. The experiments conducted have shown good agreement with the theory. For Doppler-

anemometer measurements, the production of defined particles and their simultaneous measuring is imperative, for not overstepping the boundaries for the application of the differing particle materials for the various flow problems and to be able to estimate the deviation from the actual flow in question. These boundaries are given by the respective flow problems and the demands of the experimentalist on the exactness of his measurements. The velocity measurement using Doppler-pictures delivers a general view of the distribution of a velocity component in the flow area in one picture, although at the cost of high exactitude. It is frequently just the knowledge of this distribution which is of interest. A more exact measurement could then be carried out in a further experiment at a chosen place. The development of this new measuring method is not yet completed, and the boundaries of sensitivity of the system have not yet been reached.

References

1. George, A., Comparaison simultanée d'un microphone interférentiel et d'un vélocimètre Doppler, ISL-Report N 605/82, Saint-Louis, 1982

2. Howard, L.N., Matthews, D.L., On the vortices produced in shock diffraction, J. Appl. Phys., Vol. 27, pp.223 - 231, 1956

3. Rott, N., Diffraction of a weak shock with vortex generation, J. Fluid Mech., Vol. 1, pp. 111 - 128, 1956

4. Smeets, G., George A., Laser-Doppler-Velozimetrie mit Hilfe eines Michelson-Interferometers mit schneller Phasennachführung, ISL-Report R 124/78, Saint-Louis, 1978

5. Smeets, G., George, A., Laser-Doppler-Velozimeter mit einem Michelson-Spektrometer, ISL-Report R 109/80, Saint-Louis, 1980

6. Oertel, H., Seiler, F., George, A., Visualisierung von Geschwindigkeitsfeldern mit Dopplerbildern, ISL-Report R 115/82, Saint-Louis, 1982

7. Oertel, H., Gatau, F., George, A., Schwankungsmessungen in der Mischungsschicht eines Überschallstrahls, ISL-Report R 110/82, Saint-Louis, 1982

8. Jäger, W., Teilchenmitführung in einem kompressiblen Wirbel, ISL-Report CO 215/83, Saint-Louis, 1983

9. Seiler, F., Jäger, W., Flow visualization with Doppler-pictures, ISL-Report CO 223/83, Saint-Louis, 1983.